Decreased miR-132 plays a crucial role in diabetic encephalopathy by regulating the GSK-3β/Tau pathway

Li Shi[1,2,3,*], Rui Zhang[2,6,7,*], Tian Li[4,*], Xue Han[5], Nannan Yuan[2,6,7], Lei Jiang[2,6,7], Huimin Zhou[1,6,7], Shunjiang Xu[2,6,7]

[1]Department of Endocrinology, The First Hospital of Hebei Medical University, Shijiazhuang 050000, China
[2]Central Laboratory, The First Hospital of Hebei Medical University, Shijiazhuang 050000, China
[3]Department of Endocrinology, The First Affiliated Hospital of Hebei North University, Zhangjiakou 075000, China
[4]School of Basic Medicine, The Fourth Military Medical University, Xi'an 710032, China
[5]Department of General Practice, Xingtai People's Hospital, Xingtai 054000, China
[6]Hebei Key Laboratory of Brain Science and Psychiatric-Psychologic Disease, Shijiazhuang 075000, China
[7]Hebei International Joint Research Center for Brain Science, Shijiazhuang 075000, China
*Equal contribution

Correspondence to: Huimin Zhou, Shunjiang Xu; **email:** zhouhuimin@hebmu.edu.cn, xushunjiang@hebmu.edu.cn

ABSTRACT

Diabetic encephalopathy (DE) is a global concern and Gordian knot worldwide. miRNA-132 (miR-132) is a class of negative gene regulators that promote diabetic pathologic mechanisms and its complications. However, the molecular mechanisms of miR-132 in DE are elusive, thus an alternative therapeutic strategy is urgently in demand. The present study explored the protective effect and the underlying mechanism of miR-132 on DE via the GSK-β/Tau signaling pathway. Experimentally, a type 2 DM rat model was developed by incorporating a high-fat diet and streptozotocin injection. Further, the DE model was screened via the Morris Water Maze test. Primary hippocampal neurons and HT-22 cells were used for *in vitro* analysis. We found that hyperglycemia exacerbates cognitive impairment in T2DM rats. When we isolated the primary hippocampus neurons, the expression of miR-132 RNA was low in both the DE hippocampus and primary neurons. GSK-3β and Tau 404 were highly expressed in injured HT-22 cells and diabetic hippocampal tissues. miR-132 downregulated the expression of GSK-3β. Besides, a binding and colocalized relationship between GSK3β and Tau was also reported. These findings suggest that miR-132 exerts protective effects from DE injury by repressing GSK-3β expression and alleviating Tau hyperphosphorylation in HT-22 cells and hippocampus tissues.

INTRODUCTION

Diabetes is a heterogeneous mix of health conditions characterized by glucose dysregulation. According to the Heart Disease and Stroke Statistics-2019 Update, a report from the American Heart Association, nearly 26, 9.4, and 91.8 million adults have diagnosed diabetes, undiagnosed diabetes, and prediabetes in the U.S., respectively. In 2017, the cost of DM was estimated at $327 billion, up by 26 % from 2012 [1]. Following a report by Cho et al., 451 million people had diabetes in 2017 globally, and the number is expected to rise to nearly 693 million by 2045 [2]. People with diabetes have an increased risk of developing several life-threatening health conditions, such as cardiovascular diseases [3], stroke [4], encephalopathy [5], nephropathy [6], cancer [7], oculopathy [8], and neuropathy [9], resulting in higher medical care costs.

Diabetic encephalopathy (DE) is characterized by the development of cognitive dysfunction, paresthesia, numbness, burning, and neuropsychiatric disabilities

[10–12]. Diabetic patients with a diagnosis of fewer than 12 months have a 10% possibility to suffer from diabetic neuropathy, which increases to as high as 50% at 25 years after diagnosis [13–16]. However, a majority of patients are, in most cases, diagnosed at the middle/advanced stage, thus fail to receive a good outcome. Due to this, novel theranostic targets should urgently be explored to improve the therapeutic effects and outcomes of DE.

MicroRNAs (miRs), firstly discovered in 2001 [17], are single-stranded RNA of 21-23 nucleotides in length. miRNAs are a class of negative gene regulators that modulate pathologic mechanisms occurring in diabetes and associated complications [18, 19]. So far, miR sequences from 271 organisms, 38,589 hairpin precursors, and 48,860 mature miRNAs have been annotated in mirBase [20]. In general, a single miRNA may target multiple genes, and vice versa, leading to a potentially complicated miRNA-mediated signaling network. Recent studies have demonstrated that miRs play important roles in cardiovascular diseases [21], stroke [22], cancer [23, 24], diabetes [25], among other complications [26]. Of note, dysregulation of miRs contributes to the development and progression of DE.

Glycogen synthase kinase-3β (GSK-3β), firstly isolated from rabbit skeletal muscle, is one of the few protein kinases that are inactivated via phosphorylation [27] (Supplementary Figure 1), it phosphorylates glycogen synthase involved in blood glucose regulation. Notably, the high expression of GSK-3β is correlated with insulin resistance and insulin deficiency. On the other hand, Alzheimer's disease (AD), a neurodegenerative disease that is pathologically characterized by typically senile plaques (SPs) formed from Aβ deposition, and neurofibrillary tangles (NFTs) composed of tau hyperphosphorylation [28]. GSK-3β plays an important role in the hyperphosphorylation of microtubule-associated protein Tau, one of the pathological features in AD. Based on a recent literature report, GSK-3β is potentially involved in the pathogenesis of DE. This has shifted much attention from researchers to explore the association of GSK-3β with the occurrence of DM [28]. In the present work, we explored whether miR-132 potentially downregulates the expression of GSK-3β in injured HT-22 cells.

RESULTS

Hyperglycemia exacerbates the cognitive damage in T2DM rats

During the diabetes modeling process, the diabetic group was highly presented with polyphagia, polydispia, polyuria, weariness, emaciation, and sallow hair, compared to the control group. Notably, 3 rats were eliminated on the 3rd day because their blood glucose level was less than 16.7 mM. Also, 5 diabetic rats succumbed to hyperglycemia.

The escape latency (EL) of the Morris water maze of 3 groups were not significantly different on the 1st-2nd day ($P > 0.05$). From the 3rd to 5th day, there was a significant difference in EL between the DE group and the control group (CG), as well as the DM group ($P < 0.05$). During the whole process, no significant difference was reported between the DM and CG groups (Figure 1A).

Besides, there was a significant difference in the distances across the platform between CG and DM, as well as the DE group ($P < 0.05$), whereas no significant difference was reported between the DM group and the DE group ($P > 0.05$, Figure 1B). The number of rats crossing the platform among the three groups showed a decreasing trend, with no statistical significance ($P > 0.05$, Figure 1C). The Morris water maze tests showed a confusing trajectory in the DE group, suggesting the rats could hardly find the platform. However, the trajectory of the CG and the DM groups was clear, whereby the rats directly migrated to the platform (Figure 1D).

miR-132 is expressed in low levels in DE rat hippocampal tissues and injured HT-22 cells

Here, 10 miRNAs related to brain-derived neurotrophic factor (BDNF) and silent information regulator 1 (SIRT1) were selected as potential AD-related miRNAs, according to the instructions of TargetScanHuman 7.0 as previously reported [29, 30]. They included: miR-132, miR-30c, miR -138, miR-124, miR-128, miR-155, miR-182, miR -103, miR -107, and miR -15b (Figure 2A, 2B and Supplementary Table 1). Of note, oxidative stress is a typical pathological alteration of diabetic encephalopathy [12]. BDNF [31] and silent information regulator 1 (SIRT1) [12] are the two known molecules associated with oxidative stress. Therefore, in our experiment, we chose the miRNAs that target BDNF and SIRT1.

We found a significant difference in miR-132 expression between the CG and DM groups, as well as the DE group in hippocampal tissues ($P < 0.01$, Figure 2C). Besides, the relative expression levels of miR-132 were lower in primary hippocampal neurons treated with mannitol, high glucose, and H_2O_2 compared to the control group ($P < 0.01$, Figure 2D).

GSK-3β and Tau404 are highly expressed in injured HT-22 cells and diabetic hippocampal tissues

We firstly explored whether there was a binding and colocalized relationship between GSK-3β and Tau 404.

Immunostaining results demonstrated that the colocalized relationship was enhanced in Con, DM, and DE groups, progressively (as evidenced by the overplay yellow areas in Merge image, Figure 3A). The IP results showed that there is a binding relationship between GSK-3β and Tau 404, notably, this relationship was enhanced in DM and DE groups (Figure 3E, 3G). Furthermore, GSK-3β and Tau 404 were highly expressed in Con, DM, and DE groups, progressively (Figure 3A, Supplementary Figure 2). Following immunoblot analysis, the expressions of GSK-3β, GSK-3β(T216), and Tau 404 were high in Con, DM, and DE groups, progressively (Figure 3B, 3C). However, the expression levels of Tau 396 and Tau 404 were similar between DM and DE groups (Figure 3B, 3C). *In vitro* analysis (mimicking) also demonstrated that the expression levels of GSK-3β were higher in Glu, AGEs, and H_2O_2 groups, than that of Con in HT-22 cells (Figure 3D, 3F).

miR-132 downregulates the *in vitro* expression of GSK-3β in injured HT-22 cells

In this experiment, synthetic miR-132 mimics, miR-con, and miR-132. were transfected into HT-22 cells (Figure 4A). Compared to the CG and miR-132 mimics, the expression level of GSK-3β was lower ($P < 0.05$, Figure 4B, 4C). Then, we optimized the concentration of H_2O_2 and AGEs in HT-22 cells and found that the relative cell viability was nearly 60% under 200 μM H_2O_2, which contributed to the cellular stress state [32] (Figure 5A). Moreover, the expression levels of GSK-3β was highest
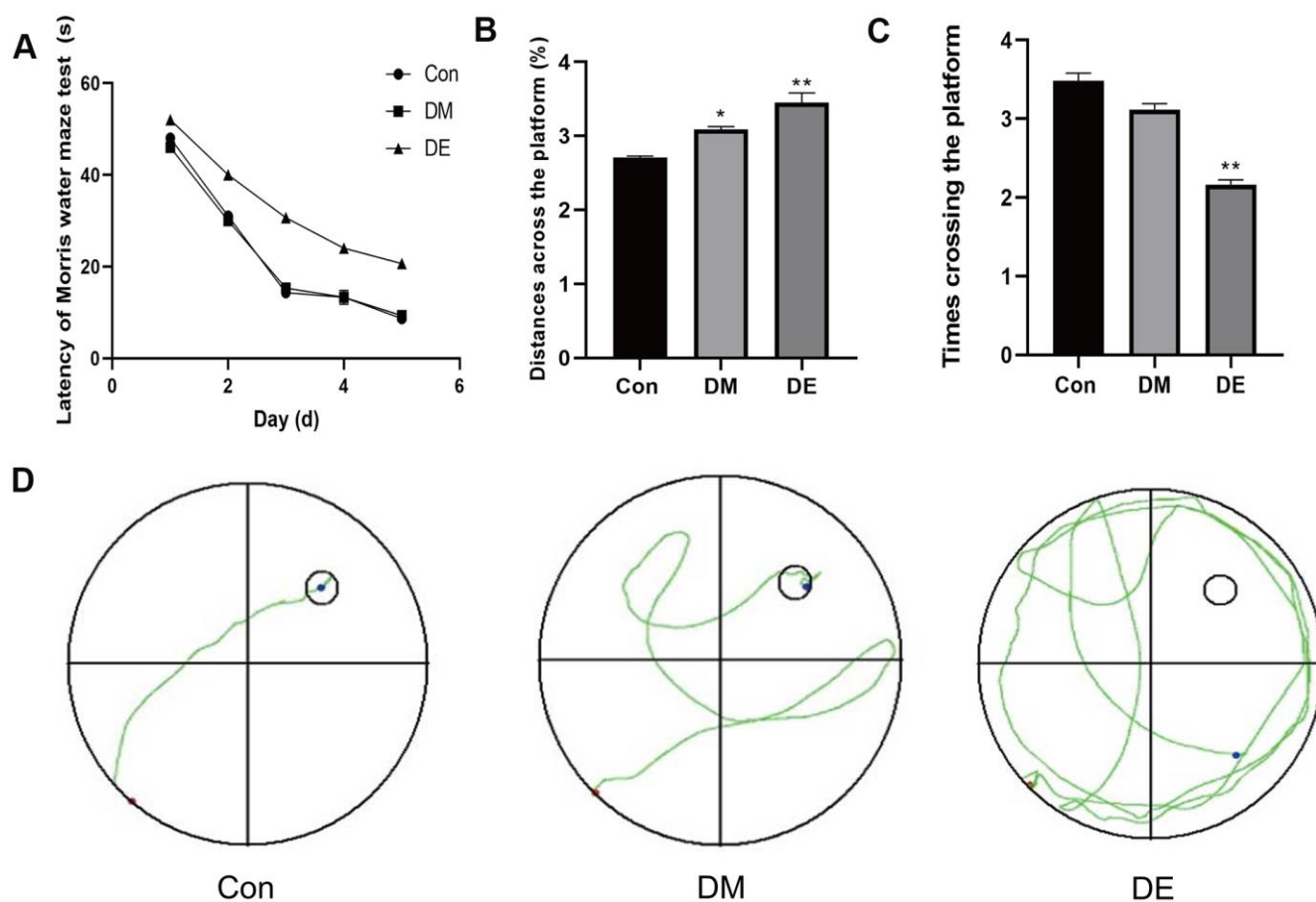

Figure 1. Hyperglycemia exacerbates the cognitive damage in T2DM rats. (**A**) The escape latency (EL) of the Morris water maze of three groups is not significantly different on the 1st-2nd day (P > 0.05). From the 3rd to 5th day, there is a significant difference of EL between the DE and CG groups, as well as the DM group (*P* < 0.05). In the entire process, there is no significant difference between the DM and CG groups. (**B**) There is a significant difference in the distances across the platform between CG and DM groups, as well as the DE group (*P* < 0.05), whereas no significant difference is evident between the DM group and the DE group. (**C**) The number of rats crossing the platform among the three groups shows a decreasing trend, with no statistical significance between Con and DM (*P* > 0.05), but there is a significance between Con and DE (*P* < 0.05). (**D**) The Morris water maze tests show a confusing trajectory in the DE group, which makes it difficult for rats to find the platform. However, the trajectory of the CG and the DM group is clear and they both directly travel to the platform. Data are presented as the mean ± SD (n = 3 per group). * P < 0.01 vs. control group, ** P < 0.05 vs. the control group, n = 5 for each group.
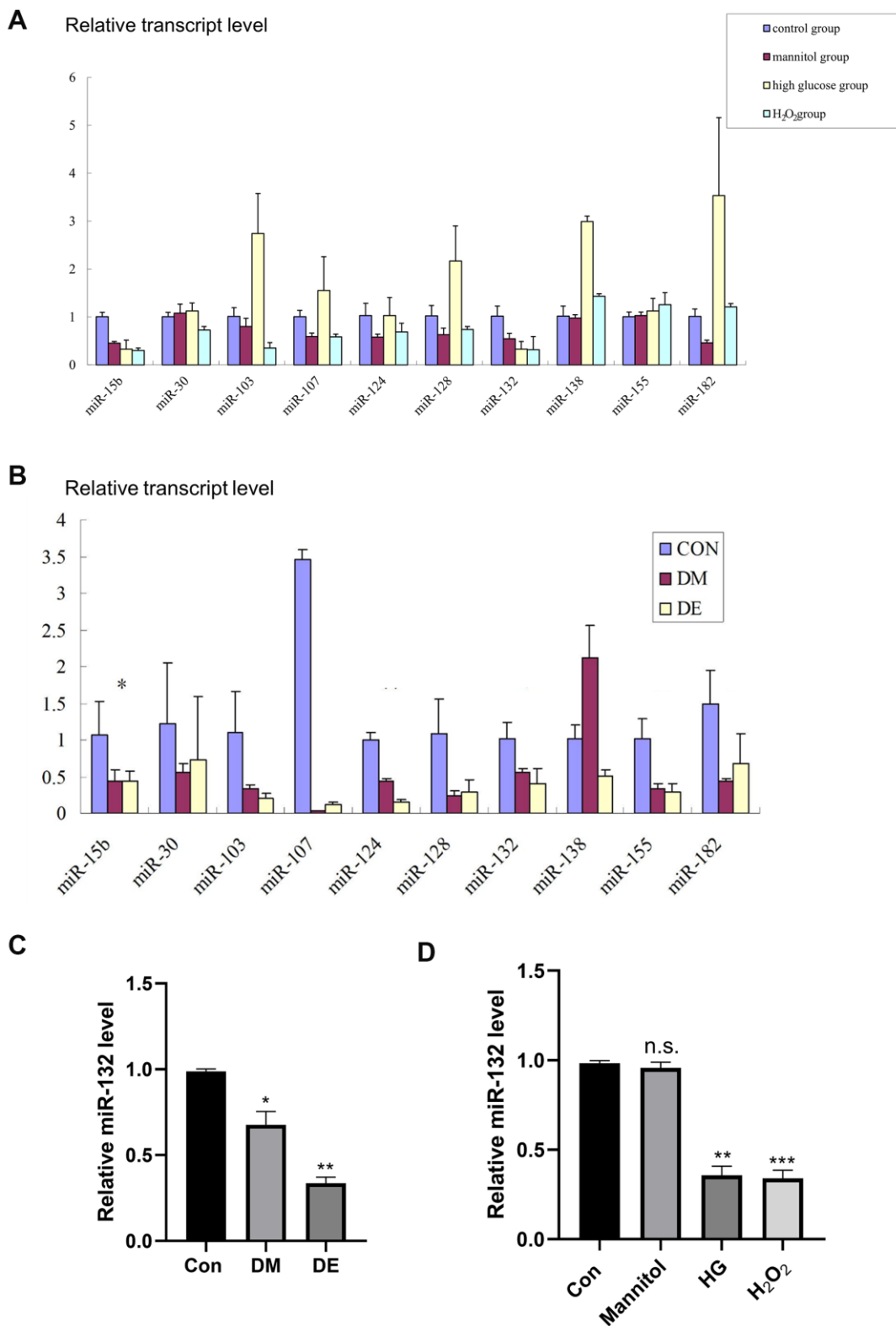
Figure 2. Low miR-132 expression in DE rat hippocampal tissues and injured HT-22 cells. (**A**) The expression levels of 10 different miRs in primary hippocampal neurons based on the qRT-PCR analysis. (**B**) The expression levels of 10 different miRs in hippocampal tissues based on the qRT-PCR analysis. *, **, and *** means $P < 0.05$, < 0.01, < 0.001 vs Con; n =3 for each group. (**C**) There is a significant difference of miR-132 between the CG and DM groups, as well as the DE group in hippocampal tissues ($P < 0.01$). (**D**) The relative expression levels of miR-132 are lower in primary hippocampal neurons treated with mannitol, high glucose, and H_2O_2 compared to the control group. Data are presented as the mean $\pm$ SD (n = 3 per group). * $P < 0.01$ vs. control group, ** $P < 0.05$ vs. the control group, n =3 for each group.

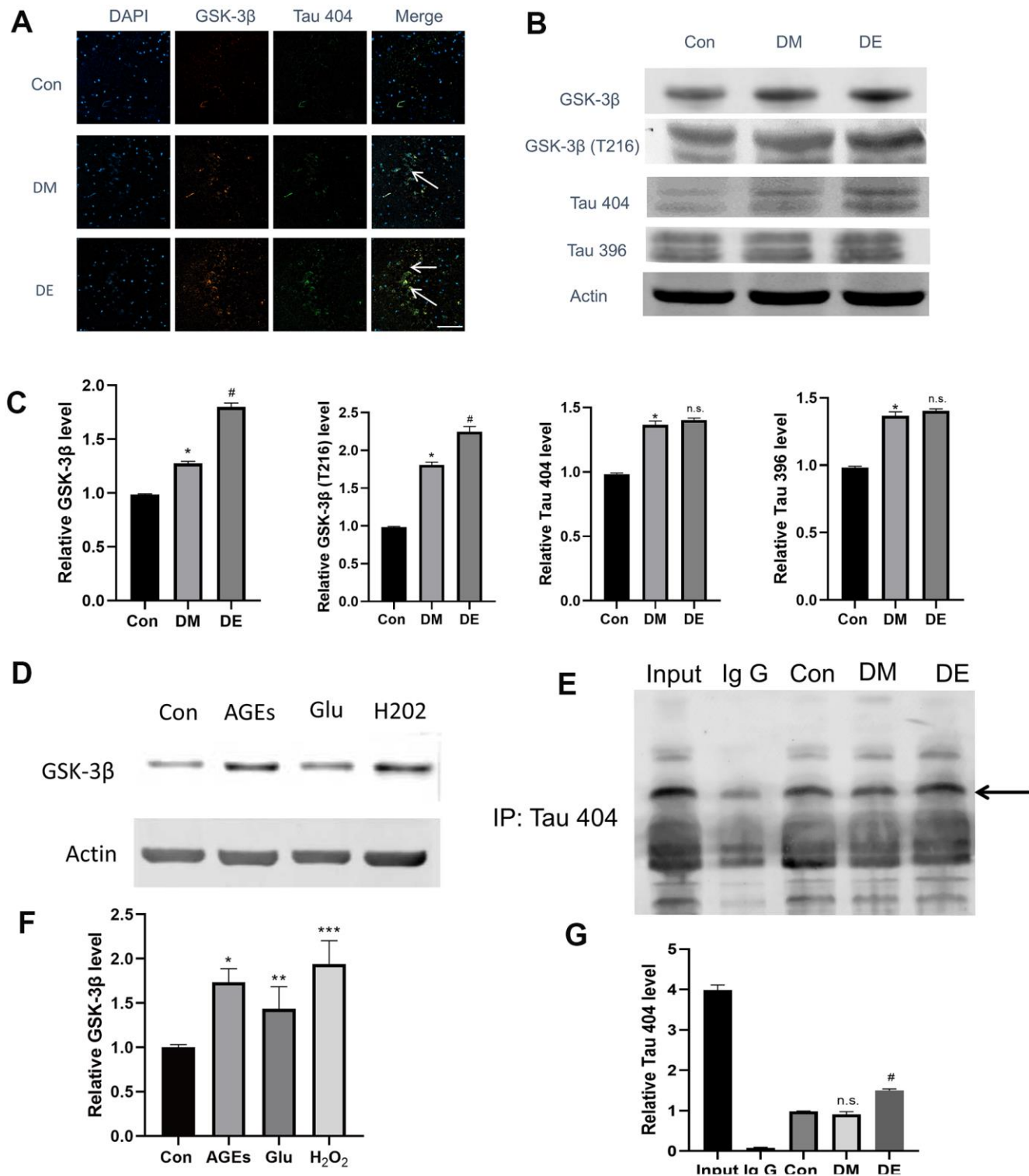**Figure 3. High expression of GSK-3β and Tau404 in injured HT-22 cells and diabetic hippocampal tissues.** (**A**) Immunostaining analysis showing the enhanced colocalized relationship in Con, DM, and DE groups, progressively (as evidenced by overplay yellow areas in Merge image). Also, GSK-3β and Tau 404 Con are highly expressed in DM, and DE groups, progressively. (**B**, **C**) The immunoblot suggesting a high expression of GSK-3β, GSK-3β(T216), and Tau 404 in Con, DM, and DE groups, progressively. However, the expression levels of Tau 396 and Tau 404 are not different between DM and DE groups. (**D**, **F**) *In vitro* experiment (mimicking) which demonstrates higher expression levels of GSK-3β in Glu, AGEs, and H_2O_2 groups, vs Con in HT-22 cells. (**E**, **G**) The IP analysis demonstrating a binding relationship between GSK-3β and Tau 404, and this relationship is enhanced in DM and DE groups. *$P < 0.05$ vs. control group, #$P < 0.05$ vs. the DM group, n =3 for each group. For Figure 3F, *, **, and *** means $P < 0.05$, < 0.01, < 0.001 vs Con; bar = 100μm.
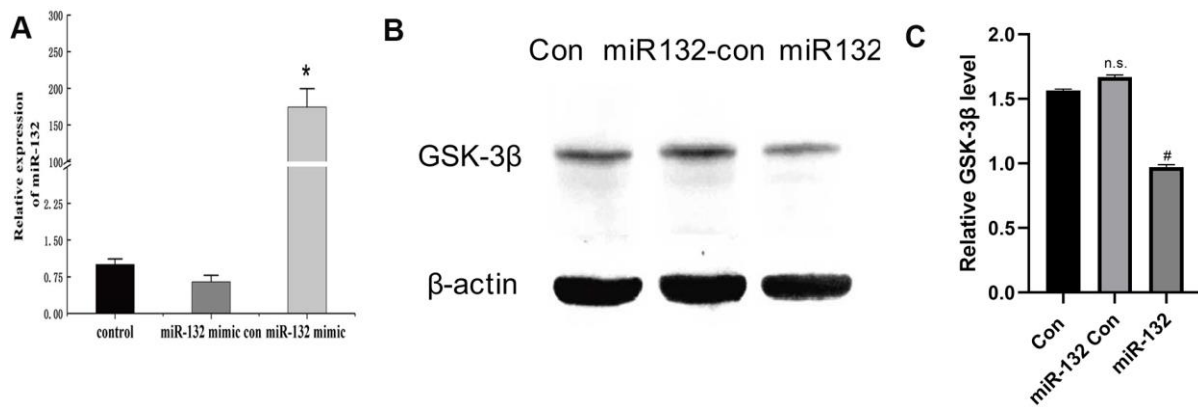
Figure 4. Successful transfection of synthetic miR-132 mimics, miR-con, and miR-132 were d into HT-22 cells. (**A**) The transfection of miR-132 is was successfully constructed in HT-22 cells. (**B**) The Western blot analysis showing that miR-132 downregulates the expression of GSK-3β. (**C**) The statistical figure of Figure 4B. *$P < 0.01$ vs. control group, #$P < 0.05$ vs. the miR-132 Con group, n = 3 for each group.
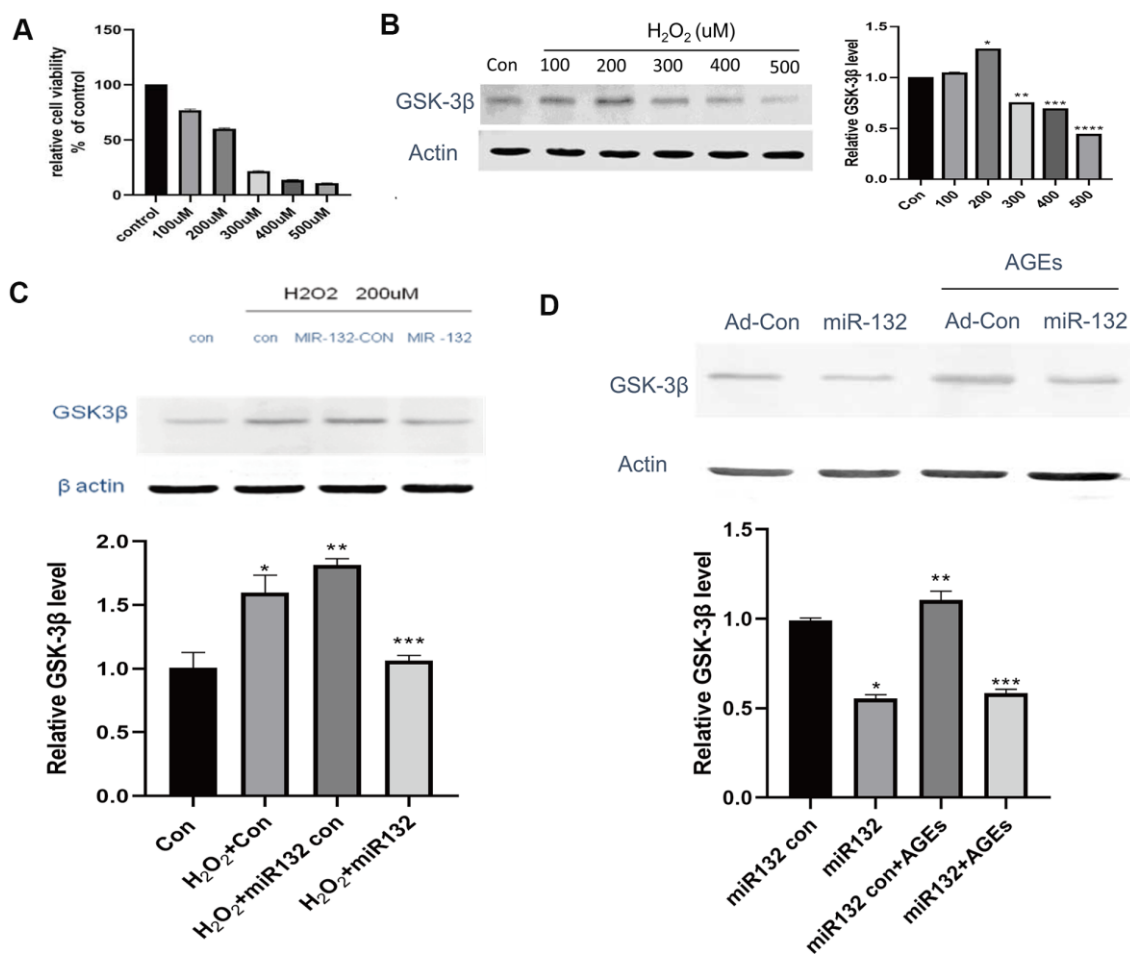

Figure 5. miR-132 downregulates the expression of GSK-3β and GSK-3β in injured HT-22 cells *in vitro*. (**A**) The relative cell viability is nearly 60% under 200 μM H_2O_2, which contributes to the cellular stress state. (**B**) The expression levels of GSK-3β among 5 groups of different concentrations H_2O_2. (**C**) miR-132 potentially reverses the upregulated levels of GSK-3β under H_2O_2 treatment. (**D**) miR-132 potentially reverses the upregulated levels of GSK-3β under the AGEs treatment. *, **, and *** means $P < 0.05$, < 0.01, < 0.001 vs Con, n = 3 for each group.

under treatment of 200 μM H_2O_2 (Figure 5B). miR-132 could reverse the upregulated levels of GSK-3β under the treatment of H_2O_2 and AGEs (Figure 5C, 5D).

DISCUSSION

Diabetic encephalopathy is characterized by the development of various conditions, including cognitive dysfunction, paresthesia, numbness, burning, and neuropsychiatric disabilities [10, 11]. Previous studies confirmed that DM patients are at high risk of developing cognitive decline in the clinic [33]. Moreover, experimental literature reports also suggested that cognitive decline exists in diabetic rats [34]. The integrity of hippocampal neurons especially the axon plays a pivotal role in DM-related cognitive damage [35]. Herein, we found that that high-fat diet and STZ-induced hyperglycemia is closely correlated with cognitive decline.

MicroRNAs are much too short to code for protein and instead play significant roles in regulating gene expression. In humans, they regulate most protein-coding genes, including genes important in diabetes and other diseases [36, 37]. In another study, Esguerra reported that the expression of miR-132 is less abundant in T2DM islets [37]. Elsewhere, Zhou and colleagues enrolled 118 gestational diabetes mellitus (GDM) women and collected their blood samples. They reported reduced expression of miR-132 in serum and placenta tissues of GDM, suggesting that serum miR-132 is a potential candidate biomarker in the diagnosis of GDM. Also, miR-132 potentially offered protection from GDM by enhancing the trophoblastic cell proliferation [36]. Additionally, Shang et al. found that overexpression of miR-132 significantly enhanced glucose-stimulated insulin secretion in insular 832/3 and 832/13 cells, and restored insulin responses to glucagon-like peptide 1 (GLP-1) in 832/13 cells [38]. However, there is no current literature report on the roles of miR-132 in DE. In our study, through an *in vitro* experiment, we discovered that miR-132 RNA expression is low in DM and DE rats, as well as the injured HT-22 cell model (Figure 2B), suggesting the potential theranostic value of miR-132 in DE.

Alzheimer's disease (AD), also regarded as Type 3 diabetes (T3D), is closely related to DM [28, 39]. In AD, GSK-3β plays an important role in the hyperphosphorylation of the microtubule-associated protein tau, which is one of the pathological features in AD. Similarly, in DM, GSK-3β is the crucial enzyme of glycogen synthesis, thereby playing a key role in blood glucose regulation. More importantly, GSK-3β is one of the key factors contributing to insulin deficiency and insulin resistance. Notably, insulin resistance is an

important hallmark of the occurrence and development of DM [28]. In this study, we demonstrated that GSK-3β is highly expressed in injured HT-22 cells and diabetic hippocampal tissues, compared to the controls. However, the overexpression of GSK-3β is positively associated with tau hyperphosphorylation.

Recently, El Fatimy's reported that miR-132 provides neuroprotection for tauopathies via multiple signaling pathways [40]. However, because their single experiment could not provide satisfactory evidence for the scientific community, we performed additional experiments for further validation of the previous findings. First, we used immunoprecipitation to directly confirm whether there is a binding relationship between GSK-3β and Tau (phosphorylation site of Tau). Second, we performed an immunofluorescence experiment to explore the colocalized relationship of GSK-3β with Tau 404. Third, since El Fatimy's work did not use 404 phosphorylation sites of Tau, we, therefore, assessed the role of Tau 404 and its relationship with GSK-3β in DE tissues.

Tau is a microtubule-associated protein that plays a role in stabilizing neuronal microtubules, thereby promoting axonal outgrowth. Structurally, tau is a natively unfolded protein, which is highly soluble and exhibits little tendency for aggregation [41, 42]. Hyper-phosphorylation and aggregation of the microtubule-associated protein tau in the brain are pathological hallmarks of a large family of neurodegenerative disorders, called tauopathies, which include Alzheimer's disease and DE [43]. Tau hyperphosphorylation is regulated by tau kinases including GSK-3β [34, 44]. Indeed, the present findings demonstrated that Tau hyperphosphorylation is higher in injured HT-22 cells and diabetic hippocampal tissues compared to the controls. Also, the overexpression of Tau 404 was associated with tau hyperphosphorylation.

Of note, DE is a global concern a Gordian knot worldwide [13]. Currently, pharmacological therapies have shown no success in preventing DE-associated diabetes. This calls for an urgent search for an alternative therapeutic strategy [35]. In the present study, we revealed that exogenous transfection of miR-132 may downregulate the expression of GSK-3β in injured HT-22 cells *in vitro*. Combining immuno-fluorescence techniques and molecular analyses *in vivo* and *in vitro*, the present study provides the first time report on protective roles of miR-132 against diabetic encephalopathy injury by repressing GSK-3β expression and alleviating Tau hyperphosphorylation. Firstly, we successfully constructed the DE model using the STZ methods and discovered that hyperglycemia exacerbates the cognitive damage in T2DM rats, as

previously reported [34]. Secondly, we isolated primary hippocampus neurons and found that expression of miR-132 RNA is low in both the DE hippocampus and primary neurons. Third, GSK-3β and Tau404 were highly expressed in injured HT-22 cells and diabetic hippocampal tissues, whereas miR-132 downregulated the expression of GSK-3β in injured HT-22 cells. Overall, these findings propose miR-132 as a new therapeutic target to alleviate the DE-induced cognitive decline, which is helpful for the clinical drug design in the management of DE and AD.

MATERIALS AND METHODS

Experimental animal and DE model

Male adult (6-8 weeks) and neonatal (1 d) Sprague Dawley (SD) rats were purchased from the Animal Experimental Center of the Hebei Medical University. Animal experiments were approved by the Instructional Animal Care and Use Committee of Hebei Medical University. Adult SD rats were fed in Animal Lab, First Affiliated Hospital of Hebei Medical University with adequate food and water under a 12-h dark-light cycle, and a temperature (23° C) and humidity (50 %) controlled room. All procedures were approved by the Animal Ethical Experimentation Committee of Hebei Medical University.

Notably, 40 rats were fed on a high-fat diet (containing 35% fat) for 4 weeks and assigned randomly to the experimental group (n=30) and control group (n=10). Streptozocin (STZ, 30 mg/kg, i.p.) and citrate buffer solution (30 mg/kg, i.p.) was administered in the experimental and control groups, respectively a 12 h fasting. Then, all rats were fed on free food and water for 72 h, after which the experimental rats were made to fast for 12 h because the model could only be successful if the caudal vein blood glucose were more than 16.7 mmo1/L (Table 1, 2).

Morris water maze

Morris water maze test was performed to evaluate the cognitive function as previously reported but with minor changes, for example, we used the method that could distinguish the DE group from the DM group [35]. In this experiment, rats injected with STZ after 22 weeks were randomly placed inside the pool at 4 possible start locations. Each rat was conditioned three times per day to let them adapt to the pool environment for 5 days, then allowed up to 5 s to locate the platform. The trial was terminated whenever the rat found the platform within 60 s. The latency was 60 s if the rats failed to find the platform within 60 s. Behaviors of rats were tracked, and we evaluated the escape latency. The

latency, distance, and swimming speed were recorded using an automated video tracking software package (NoldusEtho Vision 2.3.19, Netherland).

Antibodies and reagents

Rabbit anti-β-actin, S9-GSK-3β, T Tau 404 (1:1000), MAP-2 (1:100), mouse anti- S9-GSK-3β, and HRP-linked secondary antibodies (1:5000), FITC-linked secondary antibody (1:100) were purchased from Cell Signaling Technology (Danvers, USA). Rabbit anti-216-GSK-3β and Tau 396 were purchased from Absin (Shanghai, China).

STZ was purchased from Enzo Biochem (New York, USA). High glucose Dulbecco's modified Eagle's medium (DMEM), Neurobasal-A medium, fetal bovine serum (FBS), trypsin, Penicillin-Streptomycin-Glutamine, B-27 Supplement (50X) were purchased from Gibco (Waltham, USA). Poly-L-lysine was purchased from Sigma (USA). Triton X-100 was obtained from Bio-High Technology (Shijiazhuang, China).

Cell culture and treatment

We purchased the HT-22 cells from American Type Culture Collection (ATCC, USA). The HT-22 cells are exposed to mannitol, HG, and H_2O_2. The mannitol group was the osmotic control for HG, whereas the H_2O_2 was used to generate more reactive oxygen species [45, 46]. Neonatal rat neurons were isolated from 1-day-old SD rats. The isolation of primary hippocampal neurons was performed as previously described [40, 47–49]. Briefly, neonatal SD rats were sterilized with alcohol and sacrificed for brain tissues. The tissues were soaked in 4° C D-Hanks liquid and the hippocampus was isolated using microscope forceps under a microscope. We peeled the pia mater and blood vessels on ice. The peeled hippocampal tissues were digested by pancreatin, centrifuged, inoculated, and purified. First, we obtained the hippocampal tissues then neonatal rat hippocampal neurons as the final isolation.

To identify the primary hippocampal neurons, we used a previously described protocol but with minor modifications [50, 51]: Onto the medium, we added 3.7% paraformaldehyde and left to stand for 10min at room temperature (RT), followed by three times PBS wash, each for 5min; 2). Then, 0.1% TritonX-100 was added, left to stand for 5 min at RT, and washed in PBS thrice each for 5min at RT. Subsequently, cells were incubated with 3% Bovine Serum Albumin (BSA) confining liquid for 30min at RT, then again incubated with Rabbit anti-MAP-2 antibody (1:100) at 4° C

Table 1. The average body weight of diabetic mice.

	Diabetic group	Normal group	T value	*P*
4 weeks	362.38±64.00	366.00±84.3	−0.132	0.896
8 weeks	390.24±67.98	458.50±95.98	−2.285	0.03
12 weeks	405.24±63.92	535.50±93.76	−4.552	0.000
16 weeks	417.62±14.02	598.00±84.86	−6.585	0.000
20 weeks	420.00±75.37	658.50±78.14	−8.14	0.000
23 weeks	413.80±63.99	718.00±72.12	−11.884	0.000

Table 2. Average of blood glucose concentration (mg/dl).

	Diabetic group	Normal group	T value	P
4 weeks	334.27±70.96	122.22±12.66	13.26	0.000
8 weeks	312.34±49.81	123.12±15.06	15.94	0.000
12 weeks	331.80±35.76	129.06±20.49	16.59	0.000
16 weeks	305.82±59.72	129.96±19.06	12.25	0.000
20 weeks	324.60±44.33	131.22±15.77	17.77	0.000
23 weeks	314.83±52.33	132.30±15.35	10.73	0.000

overnight and washed in PBS thrice, each for 5 min. Further, cells were incubated with FITC-linked secondary antibody (1:100) for 30 min at RT and washed in PBS thrice, each for 5min. Then, we mounted cells using DAPI and visualized under a fluorescence microscope.

On experiment day 8, onto the primary hippocampal neurons, 200 mmol/L glucose and 100 mmol/L and mannitol were added and incubated for 24 h. This was to mimic the neuron damage *in vitro*. Then, cells were harvested for further analysis.

Immunofluorescence and immunochemistry analyses

Hippocampus was harvested, embedded in optimal cutting temperature compound, snap-frozen in liquid nitrogen-cooled isopentane, and sliced into 20-µm-thick sections using a freezing microtome. Then, we fixed the hippocampus sections with 4% paraformaldehyde and blocked with 10% serum in PBS. The sections were incubated with the Rabbit anti-GSK-3β and secondary fluorescent antibody and visualized using a confocal fluorescence microscope (Olympus Corporation, Tokyo, Japan).

Western blot and immunoprecipitation (IP) analyses

The main operating methods followed previous experiments with minor variations [52, 53] using primary antibodies listed in Section 2.2. Briefly, frozen animal heart tissues were homogenized in ice-cold riPa lysis buffer. The extracts were centrifuged for 20 min at 12,000 x g at 4° C to collect supernatants. Protein lysates (25 µg/lane) were separated in 10% SDS-PAGE and transferred onto PVDF membranes. Membranes were blocked with 7% non-fat milk for 90 min at RT and incubated with the following primary antibodies at 4° C overnight. Thereafter, membranes were incubated with an HRP-linked secondary antibody. We shipped the membranes to Quantity One 4.52 (Bio-rad Laboratories, CA, USA) for analysis. Immunoprecipitation was performed using a kit according to the manufacturer's protocol (Invitrogen, CA, USA).

miRNA transfection

miR-132 mimics (uaacagucuacagccauggucg, from 5' to 3'), miRNA mimic negative control (miR-con), were purchased from RiboBio Co., LTD (Guangzhou, China). Synthetic miR-132 mimics, miR-con, were transfected into cells using riboFECTTM CP Transfection Kit (Invitrogen, Waltham, USA) according to the manufacturer's instructions. Transfection was conducted using riboFECTTM CP Transfection Kit (Invitrogen, Waltham, USA) according to the manufacturer's instructions.

Quantitative real-time polymerase chain reaction (qRT-PCR)

Total RNA from primary cultures and mouse hippocampal slice was extracted with TRIzol Reagent (Thermo, Waltham, USA) according to the manufacturer's instruction. Reverse transcription was performed using PrimeScript RT Master Mix (TaKaRa, Kusatsu, Japan). Quantitative real-time PCR (qRT-PCR)

was prepared with the SYBR Select Master Mix (Thermo, Waltham, USA) using Bio-Rad CFX96 (Bio-Rad, CA, USA). We used the housekeeping gene β-actin as an endogenous reference. The relative gene expression values were calculated using the ΔΔCt method.

Statistical analysis

Data were expressed as mean ± SD. All statistical analyses were performed via GraphPad Prism 8 (San Diego, GraphPad Software Inc, USA), using Student's t-test for comparing two groups or one-way ANOVA. Differences with P values<0.05 were regarded as statistically significant. All experiments were performed in triplicates.

AUTHOR CONTRIBUTIONS

Conceptualization: Huimin Zhou and Shunjiang Xu; Experiments performing: Li Shi, Rui Zhang, and Xue Han. Data curation: Li Shi; Formal analysis: Rui Zhang and Tian Li; Funding acquisition: Huimin Zhou and Shunjiang Xu; Investigation: Huimin Zhou and Shunjiang Xu; Methodology: Xue Han; Project administration: Huimin Zhou and Shunjiang Xu; Resources: Huimin Zhou and Shunjiang Xu; Software: Li Shi; Supervision: Huimin Zhou and Shunjiang Xu; Validation: Nannan Yuan; Visualization: Lei Jiang; Roles/Writing - original draft: Li Shi; Writing - review and editing: Huimin Zhou and Shunjiang Xu.

ACKNOWLEDGMENTS

CONFLICTS OF INTEREST

The authors declare that they have no conflicts of interest.

FUNDING

REFERENCES

1. Benjamin EJ, Muntner P, Alonso A, Bittencourt MS, Callaway CW, Carson AP, Chamberlain AM, Chang AR, Cheng S, Das SR, Delling FN, Djousse L, Elkind MSV, et al. Heart Disease and Stroke Statistics-2019 Update: A Report From the American Heart Association. Circulation. 2019; 139:e56–e528.
https://doi.org/10.1161/CIR.0000000000000659
PMID:30700139

2. Cho NH, Shaw JE, Karuranga S, Huang Y, da Rocha Fernandes JD, Ohlrogge AW, Malanda B. IDF diabetes atlas: global estimates of diabetes prevalence for 2017 and projections for 2045. Diabetes Res Clin Pract. 2018; 138:271–81.
https://doi.org/10.1016/j.diabres.2018.02.023
PMID:29496507

3. Luo F, Das A, Chen J, Wu P, Li X, Fang Z. Metformin in patients with and without diabetes: a paradigm shift in cardiovascular disease management. Cardiovasc Diabetol. 2019; 18:54.
https://doi.org/10.1186/s12933-019-0860-y
PMID:31029144

4. Aroda V. REWIND to fast forward: time to revisit stroke prevention in type 2 diabetes? Lancet Diabetes Endocrinol. 2020; 8:90–92.
https://doi.org/10.1016/S2213-8587(19)30427-9
PMID:31924564

5. Zilliox LA, Chadrasekaran K, Kwan JY, Russell JW. Diabetes and cognitive impairment. Curr Diab Rep. 2016; 16:87.
https://doi.org/10.1007/s11892-016-0775-x
PMID:27491830

6. Wada J, Makino H. Innate immunity in diabetes and diabetic nephropathy. Nat Rev Nephrol. 2016; 12:13–26.
https://doi.org/10.1038/nrneph.2015.175
PMID:26568190

7. Holden SE. Diabetes and cancer. Endocr Dev. 2016; 31:135–45.
https://doi.org/10.1159/000439410
PMID:26824829

8. Pontiroli AE, Ceriani V, Sarro G, Micheletto G, Giovanelli A, Zakaria AS, Fanchini M, Osio C, Nosari I, Veronelli AM, Folli F; LAGB10 working group. Incidence of Diabetes Mellitus, Cardiovascular Diseases, and Cancer in Patients Undergoing Malabsorptive Surgery (Biliopancreatic Diversion and Biliointestinal Bypass) vs Medical Treatment. Obes Surg. 2019; 29:935–42.
https://doi.org/10.1007/s11695-018-3601-5
PMID:30448983

9. Giatti S, Mastrangelo R, D'Antonio M, Pesaresi M, Romano S, Diviccaro S, Caruso D, Mitro N, Melcangi RC. Neuroactive steroids and diabetic complications in the nervous system. Front Neuroendocrinol. 2018; 48:58–69.

https://doi.org/10.1016/j.yfrne.2017.07.006
PMID:28739507

10. Zhai Y, Meng X, Ye T, Xie W, Sun G, Sun X. Inhibiting the NLRP3 inflammasome activation with MCC950 ameliorates diabetic encephalopathy in db/db mice. Molecules. 2018; 23:522.
https://doi.org/10.3390/molecules23030522
PMID:29495433

11. Schemmel KE, Padiyara RS, D'Souza JJ. Aldose reductase inhibitors in the treatment of diabetic peripheral neuropathy: a review. J Diabetes Complications. 2010; 24:354–60.
https://doi.org/10.1016/j.jdiacomp.2009.07.005
PMID:19748287

12. Hu T, Shi JJ, Fang J, Wang Q, Chen YB, Zhang SJ. Quercetin ameliorates diabetic encephalopathy through SIRT1/ER stress pathway in db/db mice. Aging (Albany NY). 2020; 12:7015–29.
https://doi.org/10.18632/aging.103059
PMID:32312941

13. Liu Y, Li M, Zhang Z, Ye Y, Zhou J. Role of microglia-neuron interactions in diabetic encephalopathy. Ageing Res Rev. 2018; 42:28–39.
https://doi.org/10.1016/j.arr.2017.12.005
PMID:29247713

14. Guastella V, Mick G. Strategies for the diagnosis and treatment of neuropathic pain secondary to diabetic peripheral sensory polyneuropathy. Diabetes Metab. 2009; 35:12–19.
https://doi.org/10.1016/j.diabet.2008.09.003
PMID:19046917

15. Li T, Jiang S, Han M, Yang Z, Lv J, Deng C, Reiter RJ, Yang Y. Exogenous melatonin as a treatment for secondary sleep disorders: a systematic review and meta-analysis. Front Neuroendocrinol. 2019; 52:22–28.
https://doi.org/10.1016/j.yfrne.2018.06.004
PMID:29908879

16. Li T, Jiang S, Lu C, Yang W, Yang Z, Hu W, Xin Z, Yang Y. Melatonin: another avenue for treating osteoporosis? J Pineal Res. 2019; 66:e12548.
https://doi.org/10.1111/jpi.12548 PMID:30597617

17. Lagos-Quintana M, Rauhut R, Lendeckel W, Tuschl T. Identification of novel genes coding for small expressed RNAs. Science. 2001; 294:853–58.
https://doi.org/10.1126/science.1064921
PMID:11679670

18. Grieco GE, Brusco N, Licata G, Nigi L, Formichi C, Dotta F, Sebastiani G. Targeting microRNAs as a therapeutic strategy to reduce oxidative stress in diabetes. Int J Mol Sci. 2019; 20:6358.
https://doi.org/10.3390/ijms20246358
PMID:31861156

19. Sarkar SN, Russell AE, Engler-Chiurazzi EB, Porter KN, Simpkins JW. MicroRNAs and the genetic nexus of brain aging, neuroinflammation, neurodegeneration, and brain trauma. Aging Dis. 2019; 10:329–52.
https://doi.org/10.14336/AD.2018.0409
PMID:31011481

20. Kozomara A, Birgaoanu M, Griffiths-Jones S. miRBase: from microRNA sequences to function. Nucleic Acids Res. 2019; 47:D155–62.
https://doi.org/10.1093/nar/gky1141 PMID:30423142

21. Zhang Y, Liu X, Bai X, Lin Y, Li Z, Fu J, Li M, Zhao T, Yang H, Xu R, Li J, Ju J, Cai B, et al. Melatonin prevents endothelial cell pyroptosis via regulation of long noncoding RNA MEG3/miR-223/NLRP3 axis. J Pineal Res. 2018; 64.
https://doi.org/10.1111/jpi.12449 PMID:29024030

22. Li G, Ma Q, Wang R, Fan Z, Tao Z, Liu P, Zhao H, Luo Y. Diagnostic and immunosuppressive potential of elevated Mir-424 levels in circulating immune cells of ischemic stroke patients. Aging Dis. 2018; 9:172–81.
https://doi.org/10.14336/AD.2017.0602
PMID:29675290

23. Li S, Shan Y, Li X, Zhang C, Wei S, Dai S, Zhao R, Zhao X, Zhao L, Shan B. lncRNA SNHG5 modulates endometrial cancer progression via the miR-25-3p/BTG2 axis. J Oncol. 2019; 2019:7024675.
https://doi.org/10.1155/2019/7024675
PMID:31885582

24. Song Q, An Q, Niu B, Lu X, Zhang N, Cao X. Role of miR-221/222 in tumor development and the underlying mechanism. J Oncol. 2019; 2019:7252013.
https://doi.org/10.1155/2019/7252013
PMID:31929798

25. Feng B, Chen S, Gordon AD, Chakrabarti S. miR-146a mediates inflammatory changes and fibrosis in the heart in diabetes. J Mol Cell Cardiol. 2017; 105:70–76.
https://doi.org/10.1016/j.yjmcc.2017.03.002
PMID:28279663

26. Fan J, An X, Yang Y, Xu H, Fan L, Deng L, Li T, Weng X, Zhang J, Chunhua Zhao R. MiR-1292 targets FZD4 to regulate senescence and osteogenic differentiation of stem cells in TE/SJ/Mesenchymal tissue system via the Wnt/β-catenin pathway. Aging Dis. 2018; 9:1103–21.
https://doi.org/10.14336/AD.2018.1110
PMID:30574422

27. Baena-Díez JM, Peñafiel J, Subirana I, Ramos R, Elosua R, Marín-Ibañez A, Guembe MJ, Rigo F, Tormo-Díaz MJ, Moreno-Iribas C, Cabré JJ, Segura A, García-Lareo M, et al, and FRESCO Investigators. Risk of cause-specific death in individuals with diabetes: a competing risks analysis. Diabetes Care. 2016; 39:1987–95.
https://doi.org/10.2337/dc16-0614 PMID:27493134

28. Zhang Y, Huang NQ, Yan F, Jin H, Zhou SY, Shi JS, Jin F. Diabetes mellitus and Alzheimer's disease: GSK-3β as a potential link. Behav Brain Res. 2018; 339:57–65. https://doi.org/10.1016/j.bbr.2017.11.015 PMID:29158110

29. Garcia DM, Baek D, Shin C, Bell GW, Grimson A, Bartel DP. Weak seed-pairing stability and high target-site abundance decrease the proficiency of lsy-6 and other microRNAs. Nat Struct Mol Biol. 2011; 18:1139–46. https://doi.org/10.1038/nsmb.2115 PMID:21909094

30. Agarwal V, Bell GW, Nam JW, Bartel DP. Predicting effective microRNA target sites in mammalian mRNAs. Elife. 2015; 4:e05005. https://doi.org/10.7554/eLife.05005 PMID:26267216

31. Zeinivand M, Nahavandi A, Zare M. Deferoxamine regulates neuroinflammation and oxidative stress in rats with diabetes-induced cognitive dysfunction. Inflammopharmacology. 2020; 28:575–83. https://doi.org/10.1007/s10787-019-00665-7 PMID:31786804

32. Zhai A, Zhang Z, Kong X. Paeoniflorin alleviates H_2O_2-induced oxidative injury through down-regulation of MicroRNA-135a in HT-22 cells. Neurochem Res. 2019; 44:2821–31. https://doi.org/10.1007/s11064-019-02904-3 PMID:31728857

33. Palta P, Carlson MC, Crum RM, Colantuoni E, Sharrett AR, Yasar S, Nahin RL, DeKosky ST, Snitz B, Lopez O, Williamson JD, Furberg CD, Rapp SR, Golden SH. Diabetes and cognitive decline in older adults: the ginkgo evaluation of memory study. J Gerontol A Biol Sci Med Sci. 2017; 73:123–30. https://doi.org/10.1093/gerona/glx076 PMID:28510619

34. Zhu H, Zhang W, Zhao Y, Shu X, Wang W, Wang D, Yang Y, He Z, Wang X, Ying Y. GSK3β-mediated tau hyperphosphorylation triggers diabetic retinal neurodegeneration by disrupting synaptic and mitochondrial functions. Mol Neurodegener. 2018; 13:62. https://doi.org/10.1186/s13024-018-0295-z PMID:30466464

35. Wang S, He B, Hang W, Wu N, Xia L, Wang X, Zhang Q, Zhou X, Feng Z, Chen Q, Chen J. Berberine alleviates tau hyperphosphorylation and axonopathy-associated with diabetic encephalopathy via restoring PI3K/Akt/GSK3β pathway. J Alzheimers Dis. 2018; 65:1385–400. https://doi.org/10.3233/JAD-180497 PMID:30175975

36. Zhou X, Xiang C, Zheng X. miR-132 serves as a diagnostic biomarker in gestational diabetes mellitus and its regulatory effect on trophoblast cell viability. Diagn Pathol. 2019; 14:119. https://doi.org/10.1186/s13000-019-0899-9 PMID:31653266

37. Esguerra JL, Nagao M, Ofori JK, Wendt A, Eliasson L. MicroRNAs in islet hormone secretion. Diabetes Obes Metab. 2018 (Suppl 2); 20:11–19. https://doi.org/10.1111/dom.13382 PMID:30230181

38. Shang J, Li J, Keller MP, Hohmeier HE, Wang Y, Feng Y, Zhou HH, Shen X, Rabaglia M, Soni M, Attie AD, Newgard CB, Thornberry NA, et al. Induction of miR-132 and miR-212 expression by glucagon-like peptide 1 (GLP-1) in rodent and human pancreatic β-cells. Mol Endocrinol. 2015; 29:1243–53. https://doi.org/10.1210/me.2014-1335 PMID:26218441

39. Kandimalla R, Thirumala V, Reddy PH. Is Alzheimer's disease a type 3 diabetes? a critical appraisal. Biochim Biophys Acta Mol Basis Dis. 2017; 1863:1078–89. https://doi.org/10.1016/j.bbadis.2016.08.018 PMID:27567931

40. El Fatimy R, Li S, Chen Z, Mushannen T, Gongala S, Wei Z, Balu DT, Rabinovsky R, Cantlon A, Elkhal A, Selkoe DJ, Sonntag KC, Walsh DM, Krichevsky AM. MicroRNA-132 provides neuroprotection for tauopathies via multiple signaling pathways. Acta Neuropathol. 2018; 136:537–55. https://doi.org/10.1007/s00401-018-1880-5 PMID:29982852

41. Wang Y, Mandelkow E. Tau in physiology and pathology. Nat Rev Neurosci. 2016; 17:5–21. https://doi.org/10.1038/nrn.2015.1 PMID:26631930

42. Tapia-Rojas C, Cabezas-Opazo F, Deaton CA, Vergara EH, Johnson GV, Quintanilla RA. It's all about tau. Prog Neurobiol. 2019; 175:54–76. https://doi.org/10.1016/j.pneurobio.2018.12.005 PMID:30605723

43. Alavi Naini SM, Soussi-Yanicostas N. Tau hyperphosphorylation and oxidative stress, a critical vicious circle in neurodegenerative tauopathies? Oxid Med Cell Longev. 2015; 2015:151979. https://doi.org/10.1155/2015/151979 PMID:26576216

44. Ivashko-Pachima Y, Gozes I. NAP protects against tau hyperphosphorylation through GSK3. Curr Pharm Des. 2018; 24:3868–77. https://doi.org/10.2174/1381612824666618111210595 4 PMID:30417779

45. Fan F, Liu T, Wang X, Ren D, Liu H, Zhang P, Wang Z, Liu N, Li Q, Tu Y, Fu J. ClC-3 expression and its association with hyperglycemia induced HT22 hippocampal

neuronal cell apoptosis. J Diabetes Res. 2016; 2016:2984380.
https://doi.org/10.1155/2016/2984380
PMID:26925421

46. Tanaka T, Takei Y, Yamanouchi D. Hyperglycemia suppresses calcium phosphate-induced aneurysm formation through inhibition of macrophage activation. J Am Heart Assoc. 2016; 5:e003062.
https://doi.org/10.1161/JAHA.115.003062
PMID:27021877

47. Wang Y, Veremeyko T, Wong AH, El Fatimy R, Wei Z, Cai W, Krichevsky AM. Downregulation of miR-132/212 impairs S-nitrosylation balance and induces tau phosphorylation in Alzheimer's disease. Neurobiol Aging. 2017; 51:156–66.
https://doi.org/10.1016/j.neurobiolaging.2016.12.015
PMID:28089352

48. Meng L, Liu J, Wang C, Ouyang Z, Kuang J, Pang Q, Fan R. Sex-specific oxidative damage effects induced by BPA and its analogs on primary hippocampal neurons attenuated by EGCG. Chemosphere. 2020; 264:128450.
https://doi.org/10.1016/j.chemosphere.2020.128450
PMID:33007573

49. Zhang N, Xing Y, Yu Y, Liu C, Jin B, Huo L, Kong D, Yang Z, Zhang X, Zheng R, Jia Z, Kang L, Zhang W. Influence of human amylin on the membrane stability of rat primary hippocampal neurons. Aging (Albany NY). 2020; 12:8923–38.
https://doi.org/10.18632/aging.103105
PMID:32463790

50. Li C, Tang Y, Yang J, Zhang X, Liu Y, Tang A. Sub-chronic Antipsychotic Drug Administration Reverses the Expression of Neuregulin 1 and ErbB4 in a Cultured MK801-Induced Mouse Primary Hippocampal Neuron or a Neurodevelopmental Schizophrenia Model. Neurochem Res. 2016; 41:2049–64.
https://doi.org/10.1007/s11064-016-1917-x
PMID:27097547

51. Hannan MA, Haque MN, Dash R, Alam M, Moon IS. 3β, 6β-dichloro-5-hydroxy-5α-cholestane facilitates neuronal development through modulating TrkA signaling regulated proteins in primary hippocampal neuron. Sci Rep. 2019; 9:18919.
https://doi.org/10.1038/s41598-019-55364-8
PMID:31831796

52. Yang Y, Fan C, Wang B, Ma Z, Wang D, Gong B, Di S, Jiang S, Li Y, Li T, Yang Z, Luo E. Pterostilbene attenuates high glucose-induced oxidative injury in hippocampal neuronal cells by activating nuclear factor erythroid 2-related factor 2. Biochim Biophys Acta Mol Basis Dis. 2017; 1863:827–37.
https://doi.org/10.1016/j.bbadis.2017.01.005
PMID:28089584

53. Chang P, Zhang X, Zhang M, Li G, Hu L, Zhao H, Zhu X, Wu J, Wang X, Wang K, Zhang J, Ren M, Chen B, et al. Swimming exercise inhibits myocardial ER stress in the hearts of aged mice by enhancing cGMP-PKG signaling. Mol Med Rep. 2020; 21:549–56.
https://doi.org/10.3892/mmr.2019.10864
PMID:31974605
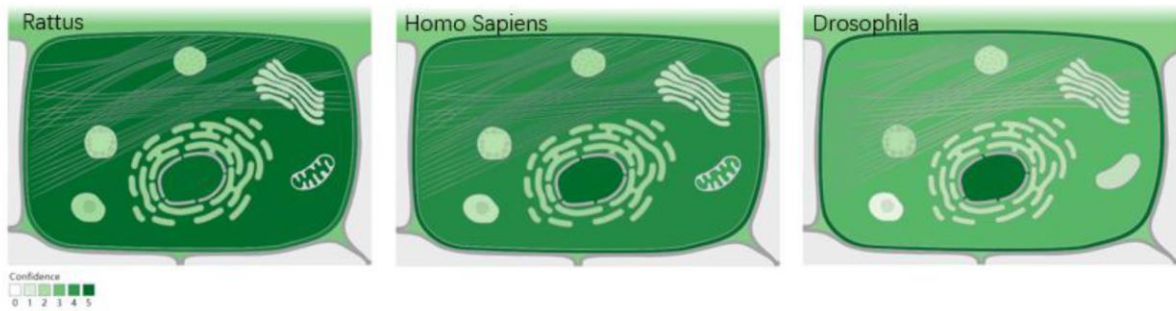
Supplementary Figure 1. Protein expression of GSK-3β in Rattus, Homo Sapiens, and Drosophila.
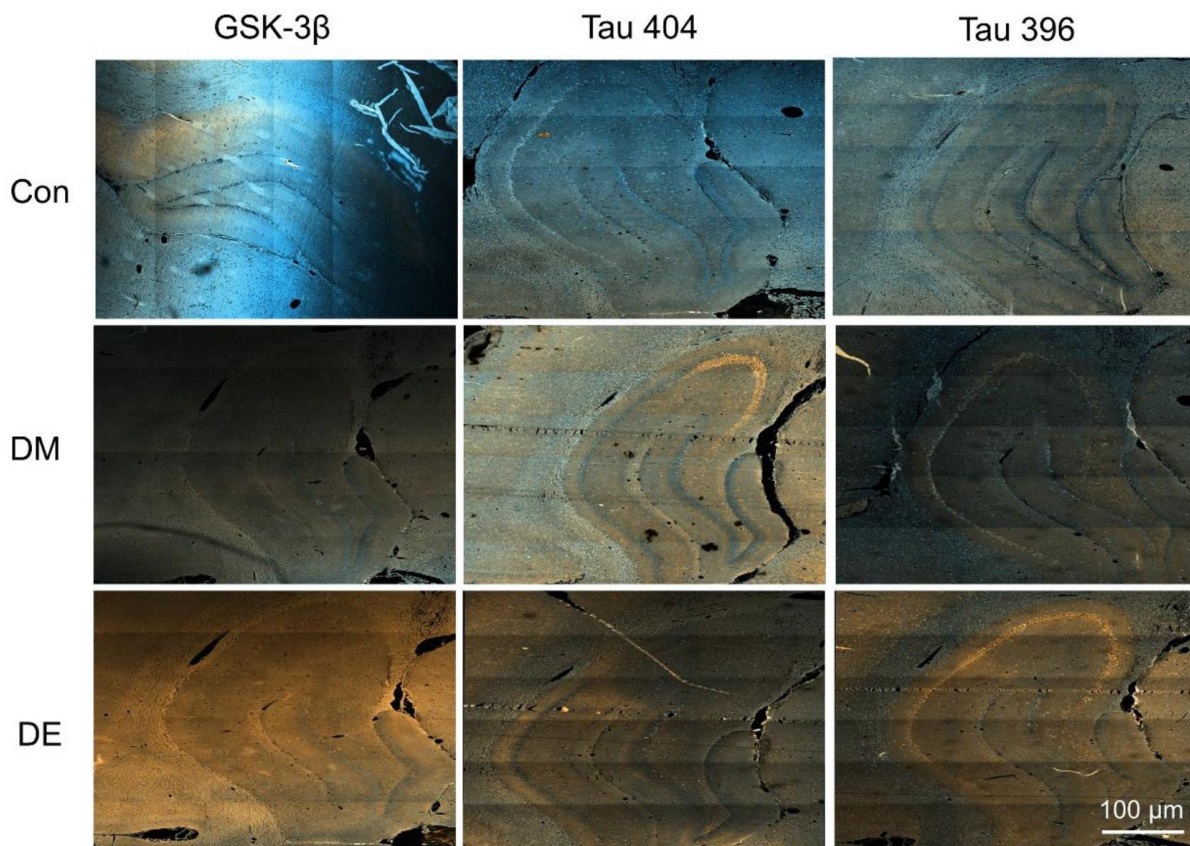
Supplementary Figure 2. The immunochemistry results of GSK-3β, Tau 404, and Tau 396 in Con, DM, and DE groups.

Supplementary Table

Supplementary Table 1. Sequence information of miRs.

Gene	Primer (5'-3')
miR-15b	UAGCAGCACAUCAUGGUUUACA
miR-30	CUGGGAGAGGGUUGUUUACUCC
miR-103	AGCAGCAUUGUACAGGGCUAUGA
miR-107	AGCUUCUUUACAGUGUUGCCUUGU
miR-124	UAAGGCACGCGGUGAAUGCC
miR-128	UCACAGUGAACCGGUCUCUUU
miR-132	UAACAGUCUACAGCCAUGGUCG
miR-138	GCUAUUUCACGACACCAGGGU
miR-155	CUCCUACCUGUUAGCAUUAAC
miR-182	CGAAUCAUUAUUUGCUGCUCUA